Research Square

Preprints are preliminary reports that have not undergone peer review.
They should not be considered conclusive, used to inform clinical practice,
or referenced by the media as validated information.

Physicochemical Properties, Structural Characteristics, and In Vitro Bioactivities of Polysaccharides from Pleurotus citrinopileatus Residue: Comparison of Six Extraction Protocols

Kunpeng Lu
Jilin Agricultural University
Yao Zhang
Jilin Agricultural University
Xinran Liu
Jilin Agricultural University
Linna Du
Jilin Agricultural University
Yuting Li
Jilin Agricultural University
Lili Guan
llguan@jlau.edu.cn

Jilin Agricultural University https://orcid.org/0000-0003-0800-5829

Research Article

Keywords: Polysaccharide extraction, Mushroom residue, Structure-function relationships, Emulsifying properties, Anti-oxidant activity, Immunomodulatory activity.

Posted Date: November 23rd, 2026

DOI: https://doi.org/10.21203/rs.3.rs-11425114/v1

License: This work is licensed under a Creative Commons Attribution 4.0 International License.
Read Full License

Physicochemical Properties, Structural Characteristics, and *In Vitro* Bioactivities of Polysaccharides from *Pleurotus citrinopileatus* Residue: Comparison of Six Extraction Protocols

Kunpeng Lu[1], Yao Zhang[1], Xinran Liu[1], Linna Du[1], Yuting Li[1,*], Lili Guan[1,*]

[1] College of Life Sciences, Engineering Research Center of Bioreactor and Pharmaceutical Development, Ministry of Education, Jilin Agricultural University, Changchun 130118, P. R. China

* Corresponding author: Yuting Li and Lili Guan

E-mail: liyuting2002@163.com, llguan@jlau.edu.cn

Abstract

Purpose: Pleurotus citrinopileatus residue (PcR) is an underutilized by-product of the mushroom industry. This study aimed to evaluate six extraction protocols for valorizing PcR into bioactive polysaccharides (PcRPs).

Methods: Six PcRP fractions were isolated using hot water, acid, ultrasound, alkali, hot alkali, and sequential acid–alkali extraction. Their physicochemical properties, structural features, functional properties, and in vitro bioactivities were systematically characterized.

Results: Extraction methods did not change monosaccharide types but altered molar ratios, molecular weight, and functional properties. AE-PcRP gave the highest yield (3.50%) and polysaccharide content (91.13%); UAE-PcRP showed the best water- and oil-holding capacity; HBE-PcRP exhibited the strongest macrophage immunomodulatory activity, increasing NO, ROS, IL-6, TNF-α, and IL-1β secretion.

Conclusion: The extraction method critically determines the functional profile of PcRPs. HBE-PcRP is a promising candidate for functional food and feed additives.

Keywords: Polysaccharide extraction; Mushroom residue; Structure-function

relationships; Emulsifying properties; Anti-oxidant activity; Immunomodulatory activity.

1. Introduction

Mushroom residue (MR), the substrate remaining after edible fungus harvest, is a valuable agricultural by-product rich in cellulose, hemicellulose, lignin, mycelium, polysaccharides, proteins, amino acids, and trace elements [1]. With the large-scale cultivation of edible fungi, the annual output of MR is substantial [2]. The lack of sustainable disposal strategies for MR poses a significant constraint on the growth of the mushroom industry [3]. Therefore, there is an urgent need to develop value-added products from MR to achieve its more efficient utilization [4]. Polysaccharides extracted from MR, as important bioactive components, retain many of the biological activities found in the original mushrooms, including anti-oxidant, anti-inflammatory, and immunomodulatory properties [5]. Consequently, the extraction of polysaccharides from MR represents a common and efficient strategy for valorizing this by-product into high-value bioproducts [6].

Pleurotus citrinopileatus (*P. citrinopileatus*), a commercially significant Basidiomycete widely cultivated in China and other Asian countries, exhibits anti-tumor, anti-oxidant, hepatoprotective, anti-inflammatory, anti-obesity, anti-hypertensive, and immunomodulatory effects [1-5]. *P. citrinopileatus* generates a large amount of post-harvest residue, *P. citrinopileatus* residue (PcR). PcR includes mycelium equivalent to nearly half of the fruiting body biomass, as well as residual polysaccharides, proteins, amino acids, and trace elements. Currently, PcR is largely underutilized, often discarded or used in low-value applications, leading to both resource waste and environmental pollution, similar to the situation of mushroom residue in the overall edible fungus industry.

P. citrinopileatus polysaccharides (PcRPs) possess multiple activities, including anti-oxidant, anti-tumor, anti-inflammatory, and immunomodulatory activities [12, 13]. However, research on polysaccharides derived from PcR (PcRPs) remains scarce. Most existing studies on PcR extraction focus on fruiting bodies and mycelia, lacking

mature protocols for extracting and characterizing bioactive polysaccharides from PcR.

The extraction method is a critical determinant of the yield, structural characteristics, and bioactivity of polysaccharides. Currently, the primary techniques for extracting polysaccharides from edible mushrooms are limited to hot water extraction (HWE) method, which is simple but relatively inefficient; ultrasound-assisted extraction (UAE) method, which enhances yield via cavitation effects. Meanwhile, polysaccharides obtained through UAE often exhibit good anti-oxidant activity [6]. Acid-assisted extraction (AE) method was used to investigate the effect of acid hydrolysis on polysaccharide yield and molecular weight reduction, polysaccharides obtained by AE have the effect of alleviating oxidative stress in mice [7-8]. Alkali extraction (BE) method and hot alkali extraction (HBE) method were designed to study the combined effects of alkaline pH and temperature on the extraction of tightly bound polysaccharides. Moreover, polysaccharides obtained by AE exhibit enhanced immunomodulatory and anti-tumor activities [9]. Despite the importance of method selection, systematic studies evaluating how these different extraction techniques influence the properties of PcRPs are lacking. Consequently, this knowledge gap restricts the rational selection of extraction protocols tailored to specific functional applications of PcRPs.

In the present study, polysaccharides from PcRPs were isolated using six distinct methods: HWE, AE, UAE, BE, HBE, and ABE. The structural properties of the obtained PcRPs were characterized by high-performance gel permeation chromatography (HP-GPC), Fourier-transform infrared spectroscopy (FT-IR), scanning electron microscopy (SEM), Congo red assay, iodine-potassium iodide (I_2-KI) test, thermogravimetric analysis (TGA), and differential scanning calorimetry (DSC). Furthermore, functional properties, including water-holding capacity (WHC), oil-holding capacity (OHC), emulsifying and foaming properties, biocompatibility, and *in vitro* bioactivities, were evaluated. This work aims to provide a scientific foundation for the efficient utilization of PcR and to support the development of PcRP-based functional products.

2. Materials and methods

2.1 Materials and reagents

1,1-diphenyl-2-picrylhydrazyl (DPPH) was obtained by Yuanye Bio-Technology Co., Ltd. (Shanghai, China). 2,2′-azino-bis (3-ethylbenzothiazoline-6-sulfonic acid) (ABTS) was supplied by Aladdin Biotechnology Co., Ltd. (Shanghai, China). Ascorbic acid (Vc), quercetin and gallic acid were supplied by Solarbio Biotechnology Co., Ltd. (Beijing, China). Lipopolysaccharide (LPS, Sigma L2630) was purchased from Sigma (St. Louis, MO, USA). The sterile defibrinated sheep blood (lot number: JS16086) was purchased from Jvshi Biotechnology Co., Ltd. (Henan, China). Griess reagent (G4410) was supported by Beyotime Biotechnology Co., Ltd. (Shanghai, China) for detecting the nitric oxide (NO) level. Interleukin-6 (IL-6) and tumor necrosis factor-α (TNF-α) ELISA kits were purchased from Bioswamp Biotechnology (Wuhan, China). Dextran standards were obtained by the National Institute of Metrology, NIM. All chemicals and reagents in the current study were analytical grade.

2.2 Extraction procedure

2.2.1 HWE method

PcR was boiled for 2 h at 90 ℃ with deionized water in a material-liquid ratio of 1:50 (w/v) (1 g : 50 mL) [10]. The filtrate was concentrated, and then absolute ethanol was added to a final concentration of 75% (v/v) to precipitate at 4 ℃ overnight. The precipitate was redissolved in deionized water, deproteinized by Sevag reagent at 1/4 volume, and then dialyzed with a membrane cutoff of 7–14 kDa against running water for 2 d and against deionized water for 2 d, with the water changed every 2 h. HWE-PcRP was obtained after freeze-drying. (**Fig.1**)

2.2.2 UAE method

UAE-PcRP was extracted following the procedure for HWE-PcRP, except that the extraction was conducted in continuous operation mode at an ultrasonic power of 200 W and 50 ℃ for 2 h in an ultrasonic cleaning machine (KQ-500DE, Kunshan,

China), followed by the same precipitation, deproteinization, and dialysis steps as described in Section 2.2.1.(**Fig.1**)

2.2.3 AE method

AE-PcRP was extracted with 0.4% HCl solution for 2 h at 50 ℃ in a material-liquid ratio of 1:50 (w/v) after deproteinization, dialysis, and freeze-drying. (**Fig.1**)

2.2.4 BE method

BE-PcRP was isolated with 0.1 M NaOH solution (pH 10) for 2 h at 50 ℃ in a material-liquid ratio of 1:50 (w/v) after deproteinization, dialysis, and freeze-drying. (**Fig.1**)

2.2.5 ABE method

PcR powders were soaked in 0.4% HCl solution at 28 ℃ for 40 min with a ratio of 1 : 30 (w/v). After deproteinization, dialysis, and lyophilization, the crude polysaccharide powder was extracted again with 0.1 M NaOH solution (pH 8.0) for 10 min at 32 ℃ according to the procedure for BE-PcRP to obtain ABE-PcRP [11]. (**Fig.1**)

2.2.6 HBE method

HBE-PcRP was extracted according to the extraction procedure of HWE-PcRP. The only difference was that 0.1 M NaOH solution (pH 8.0) was used instead of deionized water.(**Fig.1**)

HBE used 0.1 M sodium hydroxide at 90 ℃ (pH 8.0) for 2 h, while traditional BE used 0.1 M sodium hydroxide at 50 ℃ (pH 10) for 2 h. The key operational difference between the two lay in the combination of temperature and pH: HBE employed a higher temperature (90 ℃) but a lower pH (8.0), whereas BE used a moderate temperature (50 ℃) but a higher pH (10). This design aimed to evaluate the effects of heat treatment and alkaline conditions on polysaccharide extraction efficiency and structural properties.

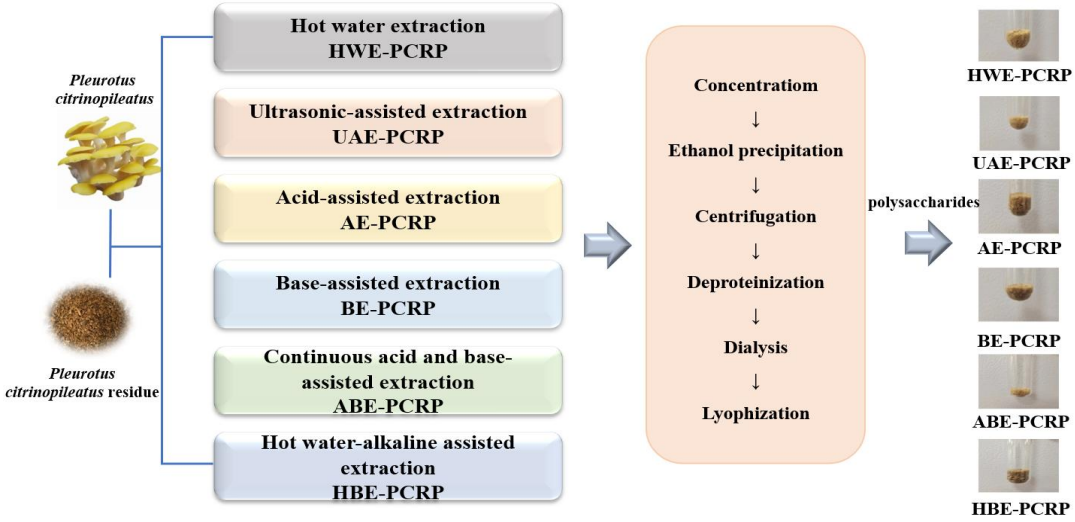

Fig.1 The preparation process of PcRPs.

2.2.7 The yield of PcRPs

The weight of PcRPs powder was determined to calculate the yield of PcRPs according to the following formula:

$$\text{Extraction yield}(\%)=\frac{m_{PCRPs}}{m_{PCR}}\times 100\%$$

Where mPcRPs and mPcR are the weights of PcRPs (g) and PcR (g), respectively.

2.3 Physicochemical properties analysis

The phenol-sulfuric acid method, Coomassie Brilliant Blue method, m-hydroxybiphenyl method, and gallic acid method were respectively utilized to measure the levels of polysaccharides, uronic acids, proteins, phenols, and reducing sugars in PcRPs [12].

2.4 Structural properties

2.4.1 Monosaccharide composition

The PcRPs were degraded with 2 M trifluoroacetic acid at 121 °C for 2 h, followed by drying under nitrogen. The resulting residue was redissolved in deionized water and filtered through a 0.22 μm microporous membrane prior to analysis. The filtrate was then analyzed on a Thermo ICS 5000^{+} ion chromatography system (Thermo Fisher Scientific, USA) equipped with a Dionex™ CarboPac™ PA20

column (150 mm × 3.0 mm, 10 μm). Data acquisition and processing were performed using Origin 2022.

2.4.2 Molecular weight (Mw)

The Mw characterization of PcRPs was performed via high-performance gel permeation chromatography coupled with an evaporative light scattering detector (HPGPC-ELSD), specifically using an Agilent 1260 Infinity ELSD system and a TSK-gel G-3000PWXL column (7.8 × 300 mm)[13]. The separation conditions were set as follows: a 10 μL sample was injected, deionized water served as the mobile phase at a flow rate of 0.6 mL/min, and the column temperature was maintained at 35 ℃. For calibration, dextran standards of varying Mw were prepared at a concentration of 10 mg/mL and employed as Mw references.

2.4.3 Fourier transform-infrared spectroscopy (FT-IR)

FT-IR spectra on a Nexus 470 FT-IR spectrometer (Equinx55, Bruce, Ettlingen, Baden-Württemberg, Germany), were recorded according to a previous study [14]. Briefly, 1 mg of dried PcRP sample was ground with 100 mg of spectroscopic-grade KBr and pressed into a transparent pellet. Spectra were acquired over the range of 4000–400 cm^{-1} at a resolution of 4 cm^{-1} with 32 scans per sample.

2.4.4 Particle size and zeta potential analysis

PcRPs solutions (1.0 mg/mL) were prepared to measure the zeta potential value and particle size on a Nanoparticle Size and Zeta Potential Analyzer (NANO ZS90, Malvern, UK) at room temperature.

2.4.5 Scanning electron microscopy (SEM)

The microstructures of PcRPs were examined using a high-resolution field-emission scanning electron microscope (FE-SEM, SU8010; Hitachi, Japan). Freeze-dried samples were mounted on conductive carbon tape and sputter-coated with a gold/palladium alloy (Au/Pd, 80:20) using a Quorum SC7620 sputter coater. Coating was carried out under high-purity argon at a sputtering current of 10 mA for 45 s, with a sample-to-target distance of 50 mm, resulting in an estimated film thickness of approximately 5–6 nm. The coated specimens were then observed with the same FE-SEM at an accelerating voltage of 10 kV. Secondary electron (SE)

images were captured at 1,000× and 5,000× magnification. The working distance was set to 8 mm. Representative images were taken from at least three random fields per sample.

2.4.6 Congo red examination and I_2-KI assay

The Congo red method was commonly used to detect the helical conformations of polysaccharides [15]. The I_2-KI assay was carried out according to a previous report [16].

2.4.7 Thermal characteristic identification

Thermal characteristics were determined according to a previous study [17]. The differential thermogravimetry (DTG) curve, which represents the degradation rate, was obtained by calculating the first derivative of the thermogravimetry (TG) curve [18].

The thermal properties of PcRPs were characterized using a TGA/DSC 1/1600 LF simultaneous thermal analyzer (Mettler Toledo, Greifensee, Switzerland).

2.4.8 X-ray diffraction (XRD) analysis

The crystal structures of PcRPs were determined using **XRD** (Rigaku SmartLab SE, Japan). Briefly, the dried sample powder was evenly spread on a glass plate. Then, it was scanned at a speed of 2 °/min within a 2θ range from 5 ° to 90 °.

2.5 Functional characterastics and biological activity assay

2.5.1 Functional characterastics analysis

OHC, WHC, foaming ability, EAI and ESI were determined according to previously reported methods with slight modifications , using an F6/10 tissue homogenizer (Shaoxing Jingxin, China) for sample preparation [19-20].

2.5.2 *In vitro* bioactivity assay

The anti-oxidant capacities of PcRPs, including those against ABTS and DPPH as well as the reducing power, were determined. Vc was selected as a positive control, as referred to in previous studies [21-22]. For the *in vitro* anti-inflammatory activity assessment of PcRPs, the inhibition of NO production and albumin denaturation was measured [23].

Albumin denaturation inhibition rate and NO inhibition rate represent the *in vitro*

anti-inflammatory activity, both of which were determined according to the aforementioned method [19].

2.5.3 Haematocompatibility assay

Haematocompatibility assay was conducted with 1% fresh sheep blood according to the reported protocol [23].

RAW 264.7 cells were cultured at 37 ℃ in an incubator with 5% CO_2 in DMEM medium containing 10% FBS and 1% penicillin-streptomycin. Cell viability after treatment with PcRPs was assessed by the CCK-8 assay.

2.5.4 *In vitro* immunomodulatory assay

RAW 264.7 cells, at a density of 1.5×10^4 cells/mL and 100 μL per well, were seeded into a black, sterile, enzyme-free 96-well plate. They were incubated overnight. Subsequently, the cells were treated with PcRPs. LPS at a concentration of 2 μg/mL was used as a control, and the treatment lasted for 24 h. After that, the cells were incubated with DCFH-DA at 37 ℃ for 30 min. Next, the cells were washed three times with serum-free DMEM and then lysed using a 1% Triton solution. Finally, the fluorescence was measured by a microplate reader (TECAN-Spark, Switzerland). The excitation wavelength was set at 488 nm and the emission wavelength at 525 nm.

The *in vitro* immunomodulatory activity of PcRPs was determined according to our previous method [24]. 100 μL of cell suspension (1.5×10^4 cells/mL) was seeded into 96-well plates for 24 h and then treated with different concentrations of PcRPs (100, 200, 400 μg/mL) for 24 h. LPS (2 μg/mL) was selected as a positive control. Furthermore, the collected cell supernatant was used to detect NO, IL-6, and TNF-α, to construct standard curves, and to measure samples according to the instructions. Absorbance was read at 450 nm using the microplate reader.

2.6 Statistical analysis

Each measurement was repeated three times, and the results were presented as the mean ± standard deviation (SD). To assess the significance among multiple samples, the Duncan test and One-way ANOVA were carried out using SPSS 26.0 software. $P < 0.05$ was considered statistically significant.

3. Result and discussion

3.1 Extraction yield and chemical components analysis

The extraction yields and chemical composition of six obtained polysaccharides (HWE-PcRP, UAE-PcRP, AE-PcRP, BE-PcRP, ABE-PcRP and HBE-PcRP) are listed in **Table 1**. The yields of PcRPs varied from 1.98 ± 0.001% to 3.50 ± 0.031% and were dependent on the different extraction methods ($P < 0.05$), while the highest yield was AE-PcRP (3.50 ± 0.031%) and the lowest yields were UAE-PcRP (1.98 ± 0.001%) and HBE-PcRP (1.98 ± 0.001%). The UAE method is generally considered to promote the extraction yield of polysaccharides [25]. However, the yield of polysaccharides extracted by the UAE method may not be the highest [10]. In the AE or BE extraction, NaOH and HCl are used to promote the release of polysaccharides during the extraction process [26]. Therefore, the extraction yields of AE method and BE method in this study were higher than those of HWE method. In addition, the yield of HBE-PcRP was the lowest, possibly due to double degradation under high temperature and alkaline conditions. The polysaccharide content of PcRPs ranged from 75.10 ± 0.013% to 91.13 ± 0.007%. The highest polysaccharide content was in AE-PcRP (91.13 ± 0.007%) and UAE-PcRP (90.80 ± 0.008%) obtained by AE and UAE methods. Hydrogen ions derived from HCl have the ability to cleave the glucosidic linkages present in the cellulose and hemicellulose components of cell walls. This cleavage process results in the diffusion of polysaccharides, which are integral parts of the cell, into the solvent medium [27]. Furthermore, the extraction yield of PcRP achieved by UAE ranked second. UAE operates based on the acoustic cavitation phenomenon. This mechanism allows it to break down cell walls, thereby enhancing the interaction between solvents and the target compounds. As a result, UAE leads to a highly efficient extraction outcome [28]. The total protein content in the PcRPs was low. The uronic acid content of HWE-PcRP (16.07 ± 0.003%) was the highest, followed by BE-PcRP (5.72 ± 0.002%), UAE-PcRP (4.42 ± 0.023%), ABE-PcRP (3.73 ± 0.001%), HBE-PcRP (3.64 ± 0.002%) and AE-PcRP (3.61 ± 0.001%), demonstrating that PcRPs were not acidic polysaccharides [29]. The total

phenolic content (TPC) was determined with values ranging from 0.58 ± 0.029 to 1.17 ± 0.038 mg GAE/g (**Table 1**).

Table 1 Extraction yield and chemical composition of PcRPs.

Physicochemical properties	HWE-PcRP	UAE-PcRP	AE-PcRP	BE-PcRP	ABE-PcRP	HBE-PcRP
Yield (%)	2.8 ± 0.002^{c}	1.98 ± 0.001^{d}	3.50 ± 0.031^{a}	3.04 ± 0.003^{b}	2.73 ± 0.306^{c}	1.98 ± 0.001^{d}
Polysaccharides (%, w/w)	87.91 ± 0.022^{b}	90.80 ± 0.008^{a}	91.13 ± 0.007^{a}	81.39 ± 0.019^{c}	75.10 ± 0.013^{d}	79.13 ± 0.006^{c}
Total phenolics (mg GAE/g)	1.17 ± 0.038^{a}	0.87 ± 0.037^{bc}	1.11 ± 0.338^{ab}	0.58 ± 0.029^{d}	1.04 ± 0.043^{ab}	0.65 ± 0.009^{cd}
Total proteins (%, w/w)	0.15 ± 0.002^{b}	0.09 ± 0.002^{e}	0.17 ± 0.007^{a}	0.13 ± 0.001^{d}	0.16 ± 0.001^{b}	0.14 ± 0.005^{c}
Uronic acids (%, w/w)	6.07 ± 0.003^{a}	4.42 ± 0.023^{b}	3.61 ± 0.001^{c}	5.72 ± 0.002^{a}	3.73 ± 0.001^{c}	3.64 ± 0.002^{c}
Particle size (nm)	399.4 ± 14.7^{c}	354.9 ± 8.1^{d}	497.6 ± 27.4^{a}	417.5 ± 5.9^{bc}	431.8 ± 9.9^{b}	269.4 ± 11.9^{e}
PDI	0.3 ± 0.1^{a}	0.3 ± 0.1^{a}	0.5 ± 0.1^{a}	0.4 ± 0.1^{a}	0.4 ± 0.1^{a}	0.3 ± 0.1^{a}
Zeta potential (mV)	-4.4 ± 0.5^{a}	-9.3 ± 1.4^{b}	-13.23 ± 1.6^{c}	-4.6 ± 1.5^{a}	-18.7 ± 2.2^{d}	-13.6 ± 0.3^{c}

Different lowercase letters indicate significant differences between different groups ($P < 0.05$).

3.2 Structural properties

3.2.1 Monosaccharide composition of PcRPs

Monosaccharide composition critically defines polysaccharide architecture and biofunctionality. While all PcRPs contained identical monosaccharide types, extraction methods significantly altered their molar ratios (**Table 2, Fig.2A**), consistent with established processing-structure relationships [30-31]. Elevated Glc in

HWE/HBE-PcRPs (13.2 mol%, 12.3 mol%) suggests enhanced β-glucan-like motifs, potentially enabling anti-bacterial activity through pathogen-associated molecular pattern (PAMP) recognition [32]. Ara represents a major structural component in PcRPs (23.0% - 33.9 mol%), with its established role in anti-oxidant efficacy extensively documented [33]. The exceptional hydroxyl radical scavenging rates observed in ABE-PcRP (84.80 ± 0.54%) and UAE-PcRP (83.97 ± 0.85%) directly correlate with their elevated Ara content. This enhanced anti-oxidant capacity is likely due to Ara's exposed hydroxyl configurations, which facilitate efficient radical neutralization through electron donation mechanisms. Critically, HWE-PcRP (13.2 mol% Glu) and HBE-PcRP (12.3 mol% Glu) exhibit superior anti-oxidant activity relative to other extracts. This enhanced capacity likely stems from structural enrichment of β-glucans, which enhance cellular anti-oxidant defenses through modulation of key enzymes including superoxide dismutase (SOD) and catalase (CAT) [34].

Table 2 Monosaccharide composition of PcRPs (mol%).

	Man	GlcA	Rha	GalA	Glc	Gal	Xyl	Ara	Fuc
HWE-PcRP	10.9	3.8	3.7	2.4	13.2	10.5	26.7	26.9	2.0
UAE-PcRP	13.0	1.7	4.6	2.3	8.6	11.3	21.7	33.9	2.9
AE-PcRP	10.9	3.3	4.1	2.4	6.3	11.2	27.9	31.9	2.1
BE-PcRP	9.8	2.9	3.7	2.2	7.1	10.5	31.6	29.1	3.1
ABE-PcRP	11.1	2.7	5.6	1.9	5.4	9.3	32.4	26.5	5.0
HBE-PcRP	11.4	3.1	4.8	2.7	12.3	8.8	31.6	23.0	2.2

3.2.2 Changes of Mw, particle size and zeta potential

Mw is an important physicochemical parameter, closely related to biological activity of polysaccharides. Polysaccharides with lower Mw were likely to exhibit higher biological activity [35]. ABE-PcRP exhibits the lowest Mw (307.69 kDa) (**Fig.2B**) yet demonstrates exceptional anti-oxidant capacity, notably an 84.80 ± 0.54% hydroxyl radical scavenging rate. This inverse relationship aligns with the observed

Mw-activity correlation pattern. The acid-mediated extraction processes (AE, ABE) induce polysaccharide chain fragmentation, reducing Mw, a structural determinant that likely enhances anti-oxidant efficacy by increasing reactive group accessibility [36-37]. Conversely, HBE-PcRP possesses the highest Mw (526.09 kDa) and displays intermediate anti-oxidant activity. This suggests compensatory mechanisms where alternative structural features collectively sustain anti-oxidant performance despite molecular size constraints.

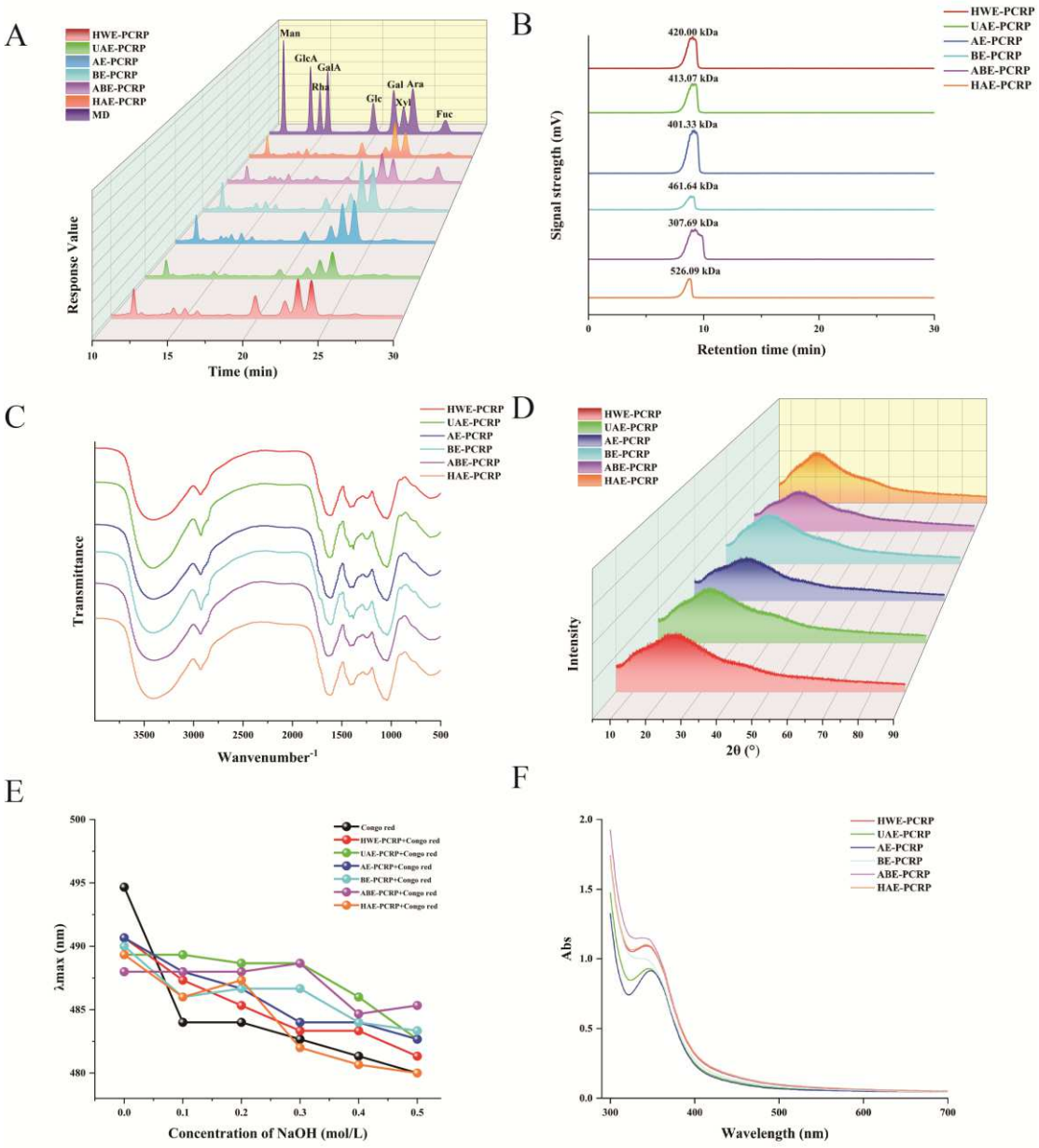

Fig.2 Changes in (A) HPAEC, (B) Mw, (C) FT-IR spectrum, (D) XRD, (E) congo red and (F) I_2-KI analysis of PcRPs.

The charge characteristics of polysaccharides can reflect the presence of anionic groups, which directly influence the stability of polysaccharide-based solutions or colloids [38]. The zeta potential values of HWE-PcRP, UAE-PcRP, AE-PcRP, BE-PcRP, ABE-PcRP, and HBE-PcRP solutions were -4.4 ± 0.5, -9.3 ± 1.4, -13.23 ± 1.6, -4.6 ± 1.5, -18.7 ± 2.2, and -13.6 ± 0.3 mV, respectively (**Table 1**). Notably, the absolute zeta potential values of HWE-PcRP, UAE-PcRP, and BE-PcRP were less than 10 mV, indicating a relatively low surface charge density [39-40].

3.2.3 FT-IR result

The FT-IR spectra (**Fig.2C**) revealed conserved functional groups across PcRPs from all extraction methods, confirming their polysaccharide nature. The broad O-H stretch at 3410 cm^{-1} and C-H vibration at 2930 cm^{-1} reflect inherent hydrophilicity and aliphatic backbone structures, respectively. Critically, the intense C=O asymmetric stretch at 1630 cm^{-1} and symmetric vibration at 1410 cm^{-1} were observed [41]. This carboxylate group density may enhance immunomodulatory potential through charge-mediated interactions with immune receptors [42]. The 1380 cm^{-1} amide signal (C-N stretch) confirms protein conjugation, consistent with the protein quantification in **Table 1**. These glycoprotein motifs could facilitate macrophage activation via TLR/lectin receptor engagement [43]. Additionally, pyranose ring signatures (C-O-C/C-O-H, 1050 cm^{-1}) indicate structural rigidity, potentially influencing polymer solubility and steric accessibility in bioactivity assays. Banana flower polysaccharides (BFPs) obtained via HWE, CAE, AAE, EAE, UAE, and HBE methods exhibit characteristic absorption signals of polysaccharides, with minimal variations in their characteristic functional groups across different extraction methods [10]. In our study, different extraction methods also did not have a significant impact on the structure of PcRPs.

3.2.4 XRD analysis

XRD is a widely utilized technique for assessing the crystallinity of samples and uncovering whether polysaccharides have crystalline or amorphous traits. It is well-recognized that the crystalline structure of polysaccharides exerts a direct impact on their physical attributes. These physical properties encompass aspects such as

tensile strength, flexibility, solubility, swelling capacity, viscosity, and opacity [44]. In addition, XRD patterns are usually determined by the structure of substance [45].

The XRD patterns of all PcRPs showed a broad diffraction peak with discernible intensity around 20 ° **(Fig.2D**), indicating their low overall crystallinity. Notably, the XRD patterns of PcRPs extracted by different methods were consistent with those of BFPs, both retaining unchanged characteristics, with relatively similar curve shapes and the presence of a broad peak near 20 °, confirming their low crystallinity [10]. This structural feature endows PcRPs with good solubility and flexibility, facilitating sufficient contact between active groups and free radicals in solution and thereby enhancing anti-oxidant efficiency.

3.2.5 Congo red analysis and I_2-KI assay

Under alkaline conditions, polysaccharides featuring a three-helix structure are capable of forming a complex with Congo red. As the concentration of the alkaline substance rises, the maximum absorption wavelength (λ_{max}) of this complex shows a redshift. This phenomenon occurs because both intermolecular and intramolecular hydrogen bonds are disrupted. Consequently, conformational changes take place, transforming the polysaccharide structure from a triple-helix to a single coil [46]. The λ_{max} of PcRPs with Congo red at various concentrations of sodium hydroxide is shown in **Fig.2E**. UAE-PcRP and ABE-PcRP showed a similar red shift in λ_{max} compared to the Congo red solution under strong alkaline conditions, suggesting that they possessed triple-helical conformations. However, the red shifts in HBE-PcRP, AE-PcRP, BE-PcRP, and ABE-PcRP were not significant, indicating that they did not possess triple-helical conformations. Currently, most known triple helix polysaccharides typically have a β-1,6 glucan or β-1,3 glucan structure [30]. However, the Glc content of UAE-PcRP and ABE-PcRP was not the highest compared to other PcRPs, but may possess a higher content of β-1,6 glucan or β-1,3 glucan structures, which will be further confirmed. The λ_{max} of PcRPs was located around 340 nm, and no absorption peak was observed at 565 nm (**Fig.2F**). These results indicate that the structural characteristics of PcRPs and TZPs are consistent, both of which are complex chain structures composed of highly branched long chains [47].

3.2.6 Surface morphology of PcRPs

The extraction and purification conditions may affect the structures, activities, and surface morphologies of polysaccharides [48]. **Fig.3** illustrates the SEM images of PcRPs extracted by HWE, UAE, AE, BE, ABE, and HBE methods at magnifications of 1.00 k and 5.00 k. Six PcRPs exhibited the fragment appearances with irregular size and shape. UAE-PcRP had uneven surfaces, presenting a tight reticulated structure. HWE-PcRP and ABE-PcRP exhibited a fine porous structure. Polysaccharides can be degraded by hydrochloric acid first and then corroded by sodium hydroxide, resulting in a sheet-like porous structure [11]. AE-PcRP exhibited irregular pores and grooves. The surface of HBE-PcRP exhibited a rich porous structure with varying pore sizes and uneven distribution, forming a complex pore network, which may be caused by high temperature and alkaline conditions [49]. The complex pore network structure can provide more attachment points for immune cells, promote material exchange and signal transmission between cells, and enhance the recognition and clearance ability of immune cells to pathogens. BE-PcRP exhibited a reticular structure with loosely filamentous cross-linking. The porous structure of polysaccharides can increase their contact area with water molecules, thereby improving their water holding capacity (WHC) [50]. A loose network architecture has a propensity to enhance the solubility of polysaccharides, thereby exposing more active groups [51]. Polysaccharides with small pore structures can promote cell attachment, proliferation, and differentiation, serving as scaffold materials for cell culture and tissue regeneration.

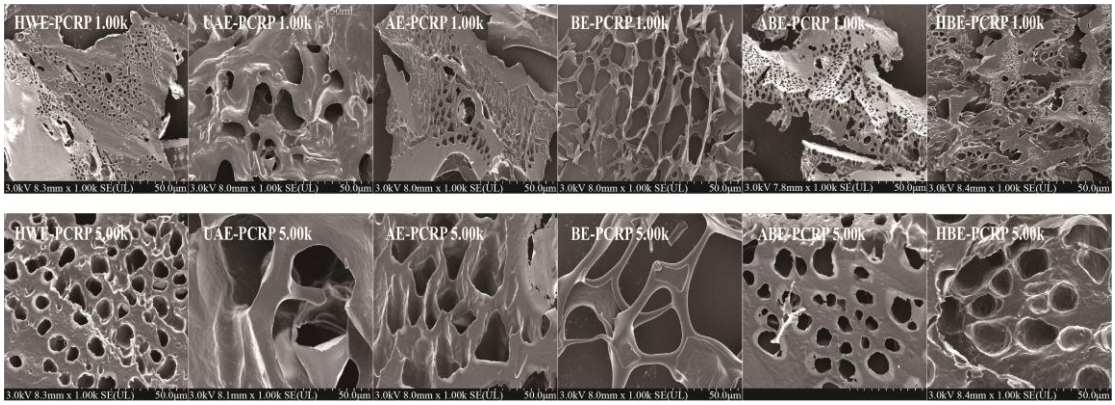

Fig.3 SEM images of PcRPs at different magnifications.

(A) 1.00 k and (B) 5.00 k.

3.2.7 Thermal stability determination of PcRPs

Thermal stability serves as a means to quantitatively identify the alterations in material quality related to dehydration, decomposition, and oxidation processes. In the context of PcRPs, it is essential to ensure both their thermal stability and biological activity. This quantification of thermal stability allows for a better understanding of how PcRPs may be influenced by heat-induced changes, while maintaining their crucial biological functions [52]. TG curves of PcRPs show relatively similar shapes depicted in **Fig.4**. The first mass loss (30–110 ℃), accounting for 14.34% and 14.43% in BE-PcRP and HBE-PcRP (the highest rates), arises from the loss of absorbed and bound water in the biopolymers [53], indicating their superior water-retention capacity. The second mass reduction (240–320 ℃) arises from polysaccharide structural decomposition [54], UAE-PcRP and ABE-PcRP presented mass losses of 78.41% and 74.37%, respectively, demonstrating better thermal stability than the other four PcRPs. However, their broadly comparable TG curves imply extraction methods had negligible influence on thermal stability. PcRPs exhibited good stability around 200 ℃ and relatively stable up to 250 ℃, supporting their applicability in various food systems.

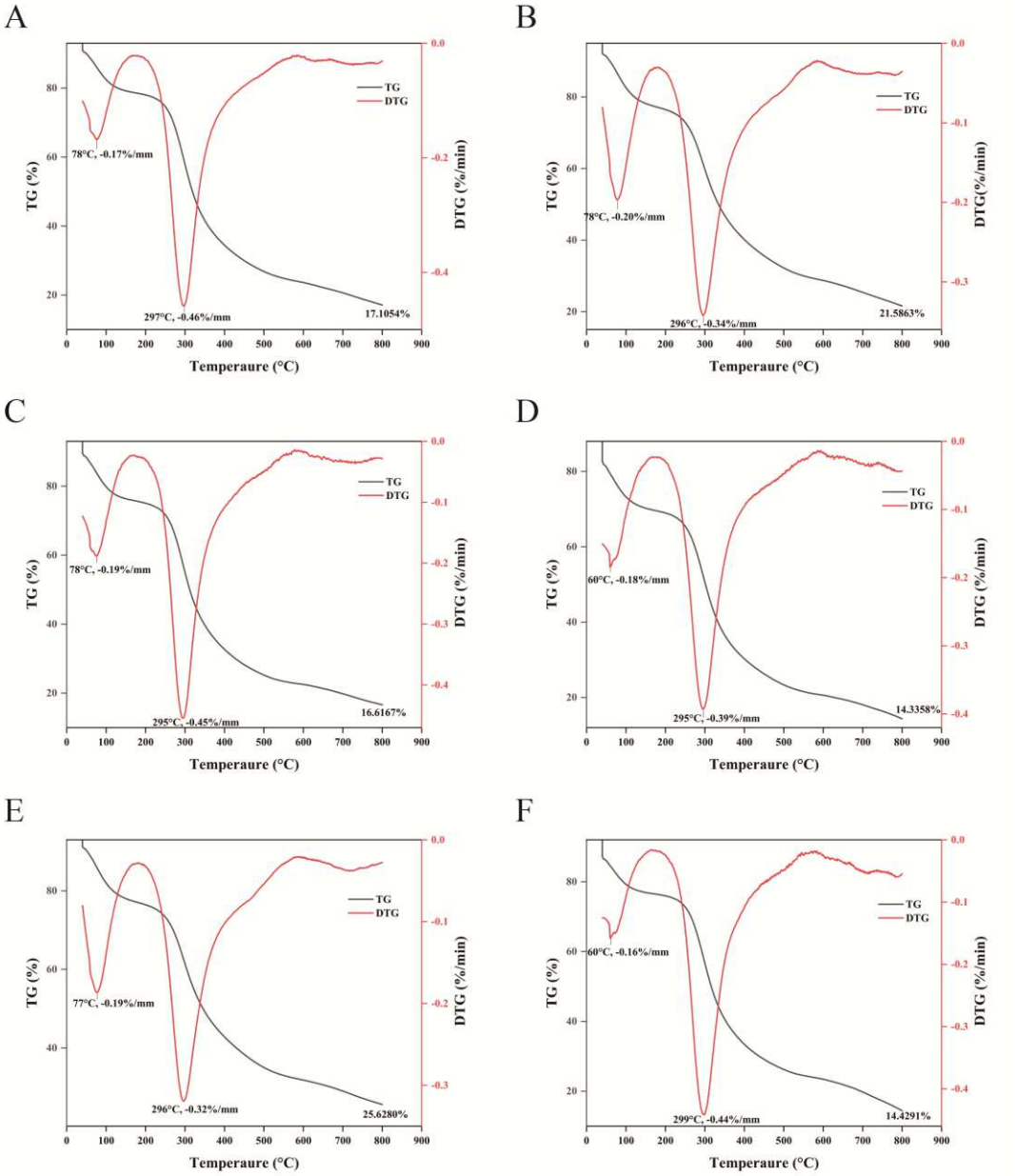

Fig.4 The thermal analysis of the PcRP extracted by different extraction methods.

(A) HEW-PcRP, (B) UAE-PcRP, (C) AE-PcRP, (D) BE-PcRP, (E) ABE-PcRP, (F) HBE-PcRP.

3.3 Functional characteristics of PcRPs

3.3.1 WHC and OHC of PcRPs

The WHC and OHC of polysaccharides can reflect their structural density and also have a significant impact on the taste, texture, and flavor of food products [55]. Different extraction methods have a significant impact on the water and oil holding capacities of PcRPs. In this study, the WHC of UAE-PcRP was the highest with 1.89 ± 0.01 g (**Fig.5A**). UAE-PcRP, AE-PcRP and BE-PcRP had higher OHC (7.45 ± 1.72,

7.56 ± 0.07, 7.89 ± 0.13 g oil/g, respectively) ($P < 0.05$) (**Fig.5A**). SEM observation revealed that UAE-PcRP had an irregular, compact honeycomb microstructure (**Fig.3**), which may enhance its water and oil-binding capacity by virtue of the tight mesh structure. Consistently, UAE-PcRP exhibited relatively high WHC and OHC compared with PcRPs from other extraction methods, supporting its potential as a stabilizer in high-fat food product development [56].

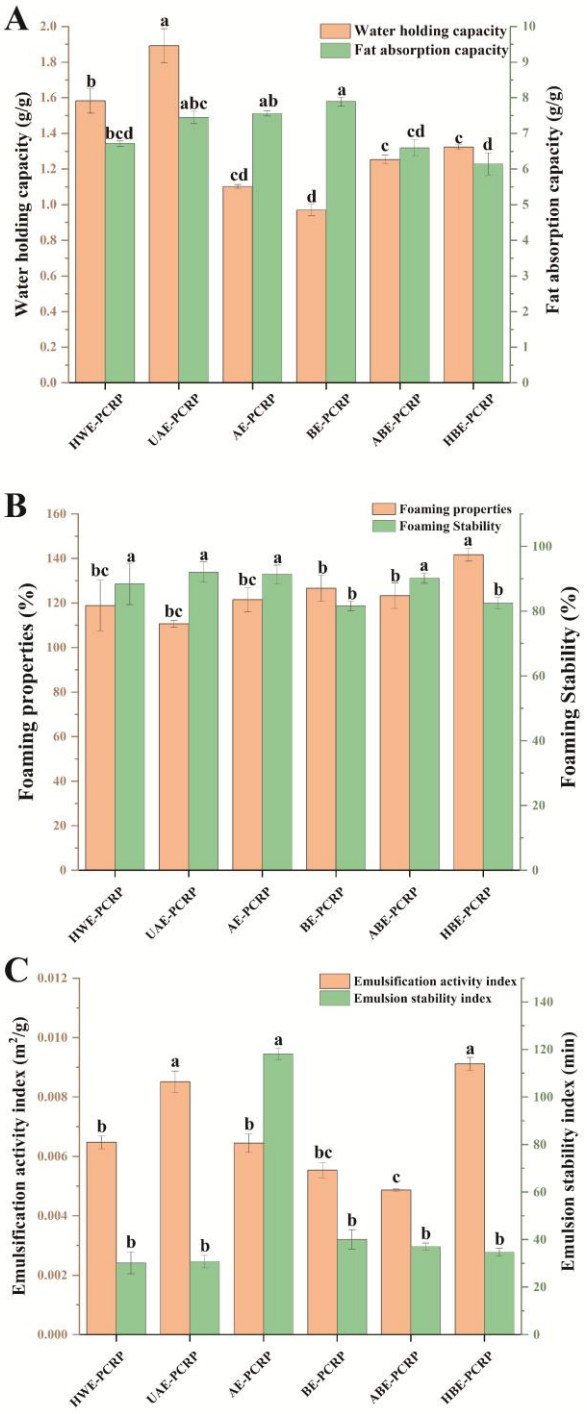

Fig.5 Functional properties PcRPs.

(A) Water holding capacity and oil holding capacity, (B) Foaming capacity and foam stability, (C) EAI and ESI.

Different lowercase letters indicate significant differences between different groups ($P < 0.05$).

3.3.2 Foaming properties of PcRPs

A blowing agent is a type of surfactant that promotes incorporation into the food matrix by lowering the interfacial tension at the gas-water interface [57]. As shown in **Fig.5**, the foaming properties and foaming stability of PcRPs prepared by different extraction methods exhibited significant differences. HBE-PcRP possessed the best foaming ability (141.67 ± 2.89 g/g) compared to the other five PcRPs (**Fig.5B**). However, HWE-PcRP, UAE-PcRP, AE-PcRP, and ABE-PcRP had better foaming stability, significantly higher than those of BE-PcRP and HBE-PcRP. In summary, UAE-PcRP may be suitable for a broader range of applications as a foaming agent in the food industry, for instance, to enhance foaming in bread and cakes, analogous to polysaccharides from ginger stems and leaves [57].

3.3.3 Emulsifying properties of PcRPs

The EAI and ESI in polysaccharides depends on complex sugar structures and hydrophobic protein interactions. The EAI and Emulsifying stability index (ESI) of polysaccharides are linked to complex sugar moieties and hydrophobic proteins [58]. Among the six different PcRPs, AE-PcRP exhibited the highest ESI (118.52 ± 2.12 g/g) (**Fig.5C**) significantly surpassing those of the PcRPs. However, UAE-PcRP and HBE-PcRP displayed the greatest EAI values, while ABE-PcRP showed the lowest EAI (**Fig.5C**). The outstanding stability of AE-PcRP renders it a promising natural emulsifier for dairy systems requiring long-term homogeneity-such as yogurt, cream cheeses, or emulsion-based beverages-where resistance to phase separation is essential.

3.4 *In vitro* bioactivities of PcRPs

3. 4.1 *In vitro* anti-oxidant abilities

The *in vitro* bioactivities of PcRPs, including anti-oxidant capacity, are influenced by chemical composition, monosaccharide profile, and Mw [59]. Obviously,

different extraction methods had significant impacts on the *in vitro* bioactivities of PcRPs (**Fig.6**). ABTS and DPPH radical scavenging activity and hydroxyl radical scavenging activity are widely used applied to evaluate the total anti-oxidant abilities of compounds [60]. Six PcRPs all showed a dose-dependant scavenging ability (**Fig.6A-C**). Regarding hydroxyl radicals, small increases in concentration at the lower end of the range brought large increases in scavenging ability for UAE-PcRP and ABE-PcRP, while similar increases brought only small increases in scavenging ability for HWE-PcRP, AE-PcRP, BE-PcRP, and HBE-PcRP. At 4 mg/mL, the scavenging abilities of UAE-PcRP and ABE-PcRP on the hydroxyl radical were 83.97 ± 0.85% and 84.80 ± 0.54%. The best ABTS radical scavenging activity was shown by the PcRP extracted by the BE method (61.97 ± 1.29%) (**Fig.6B**), while the best DPPH radical scavenging activity was shown by the PcRP extracted by the HWE method (66.21 ± 0.64%) (**Fig.6C**). The half inhibitory concentration (IC_{50}) value for hydroxyl of HWE-PcRP was the lowest (2.89 ± 0.08 mg/mL) (**Fig.6D**). HBE-PcRP and BE-PcRP possessed the lowest IC_{50} values for ABTS (4.46 ± 0.10 mg/mL each) (**Fig.6E**), while HWE-PcRP had the lowest IC_{50} value for DPPH (5.13 ± 0.10 mg/mL) **(Fig.6F**). Overall, HWE-PcRP had the highest anti-oxidant properties due to lower IC_{50} values for ABTS and DPPH radicals. PcRPs extracted via alkaline extraction (HBE/BE) methods showed exceptional ABTS radical scavenging efficiency, aligning with reports that HBE method enhances anti-oxidant properties in plant polysaccharides [61]. ABE-PcRP was thus a prime candidate for natural anti-oxidant development in food preservation or nutraceuticals, while HWE-PcRP showed promise for DPPH-targeted applications. Hence, ABE method was suggested to effectively isolate polysaccharides with strong radical-scavenging capacity from PcR.

3.4.2 *In vitro* anti-inflammatory properties

PcRPs exhibited significant anti-inflammatory activity, though efficacy varied by extraction method (**Fig.6G-H**). UAE-PcRP showed the strongest inhibition of albumin denaturation (87.5 ± 0.83%), while BE-PcRP demonstrated optimal suppression of NO production (14.91 ± 0.40%). These extraction-dependent properties highlight distinct therapeutic potential: UAE-PcRP shows promise for

applications requiring protein stabilization (e.g., biopharmaceuticals), and BE-PcRP emerges as a candidate for targeting NO-mediated inflammation.

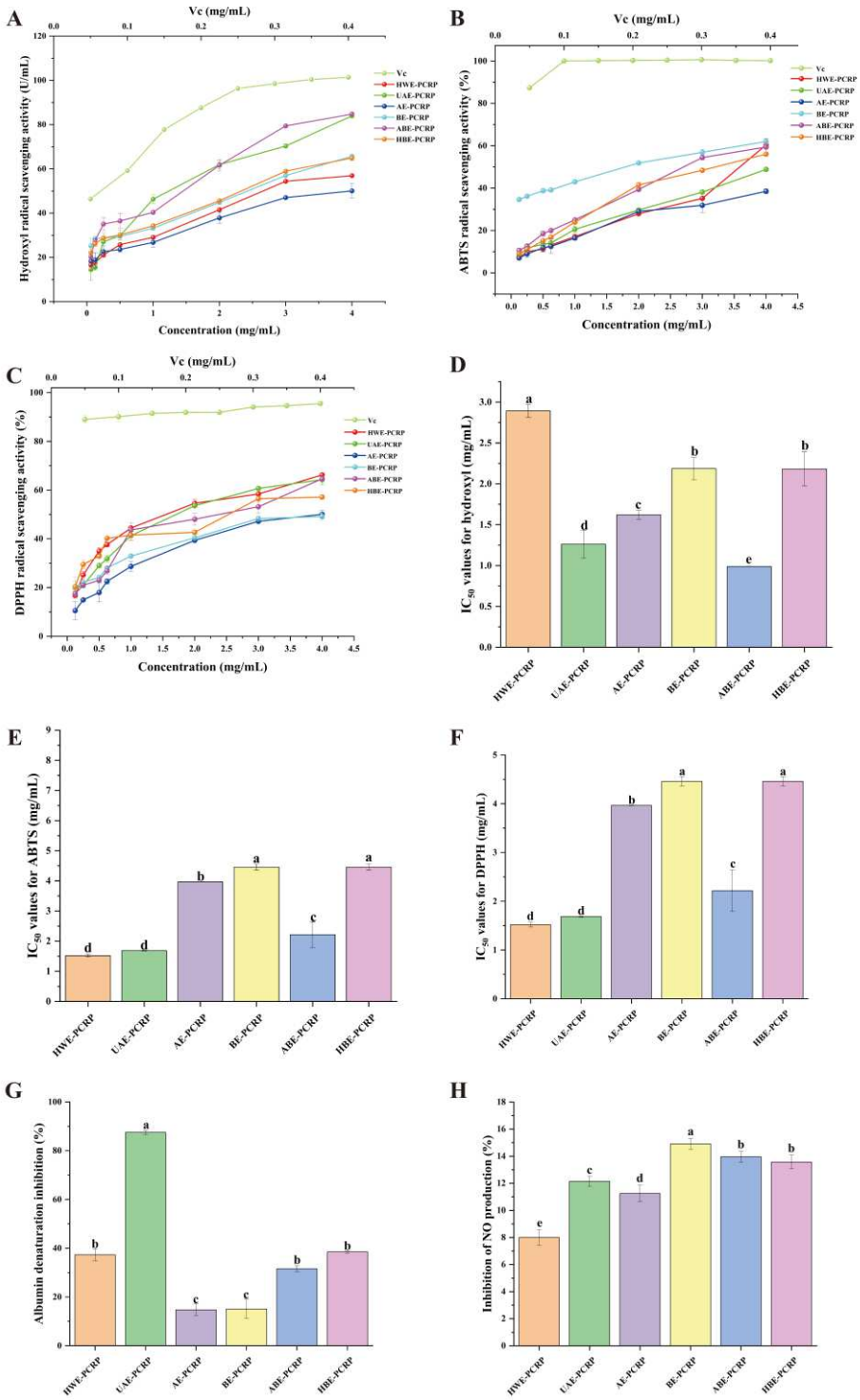

Fig.6 *In vitro* bioactivities of PcRPs.

(A) Hydroxyl radical scavenging activity, (B) ABTS radical scavenging activity, (C) DPPH radical scavenging activity, (D) IC_{50} values of hydroxyl radical scavenging, (E) IC_{50} values of ABTS radical scavenging, (F) IC_{50} values of DPPH radical scavenging, (G) Albumin denaturation

508 inhibition, (H) Inhibition of NO production.

509 *Different lowercase letters indicate significant differences between different groups ($P < 0.05$).

510 **3.4.3 *In vitro* immunomodulatory ability of PcRPs**

511 The CCK-8 assay confirmed that all PcRPs were non-cytotoxic to RAW 264.7
512 cells within the tested concentration range (**Fig.S1**). Hemolysis assays showed
513 minimal hemolysis (2-5%, **Fig.S2**), consistent with prior studies [62], confirming their
514 biocompatibility and safety for further development.

515 PcRPs significantly activated RAW 264.7 macrophages. Treatment with
516 HWE-PcRP, UAE-PcRP, AE-PcRP, and HBE-PcRP induced a dose-dependent
517 increase in NO production (**Fig.7A**). Furthermore, all PcRPs significantly enhanced
518 phagocytic activity compared to LPS (**Fig.7B**), implying a key mechanism for their
519 immune activation. PcRPs also significantly increased reactive oxygen species (ROS)
520 release relative to untreated controls (**Fig.7C**), though levels remained below those
521 induced by LPS. Moderate levels of ROS exert regulatory effects on cell proliferation,
522 differentiation, and immune function [59], Thus, ROS promotion likely contributes to
523 PcRP immunomodulation, aligning with findings on similar polysaccharides [63].
524 Cytokine analysis also revealed the potent immunostimulatory effects of LPS and
525 PcRPs. LPS significantly elevated TNF-α, IL-6, and IL-1β secretion compared to the
526 control group ($P < 0.05$). UAE-PcRP exhibited the most significant promotion of IL-6
527 secretion (172.62 ± 6.04 pg/mL) (**Fig.7D**), exceeding other PcRPs ($P < 0.05$).
528 ABE-PcRP and HBE-PcRP possessed potent stimulation of TNF-α secretion, even
529 higher than LPS ($P < 0.05$) (**Fig.7E**); yet other PcRPs showed no significant
530 stimulation of TNF-α. This phenomenon was also observed in *Sanghuangporus*
531 *vaninii* mycelium polysaccharides [64]. Six PcRPs significantly enhanced IL-1β
532 secretion compared to the control group ($P < 0.05$). ABE-PcRP and HBE-PcRP were
533 particularly effective in enhancing IL-1β secretion, inducing levels 1.19-fold and
534 1.26-fold higher than LPS, respectively (**Fig.7F**). The above data demonstrate that
535 PcRPs were biocompatible and exhibited significant *in vitro* immunomodulatory
536 activity by stimulating phagocytosis, NO production, ROS release, and cytokines
537 secretion (TNF-α, IL-6, IL-1β). *In vitro* results provide a strong theoretical basis and

direction for developing PcRPs, particularly those extracted by efficient methods like HBE, as potential immunostimulatory feed additives for livestock or aquaculture. Future work should focus on elucidating the specific immunomodulatory mechanisms using *in vitro* models and multi-omics approaches (microbiomics, transcriptomics, proteomics, metabolomics).

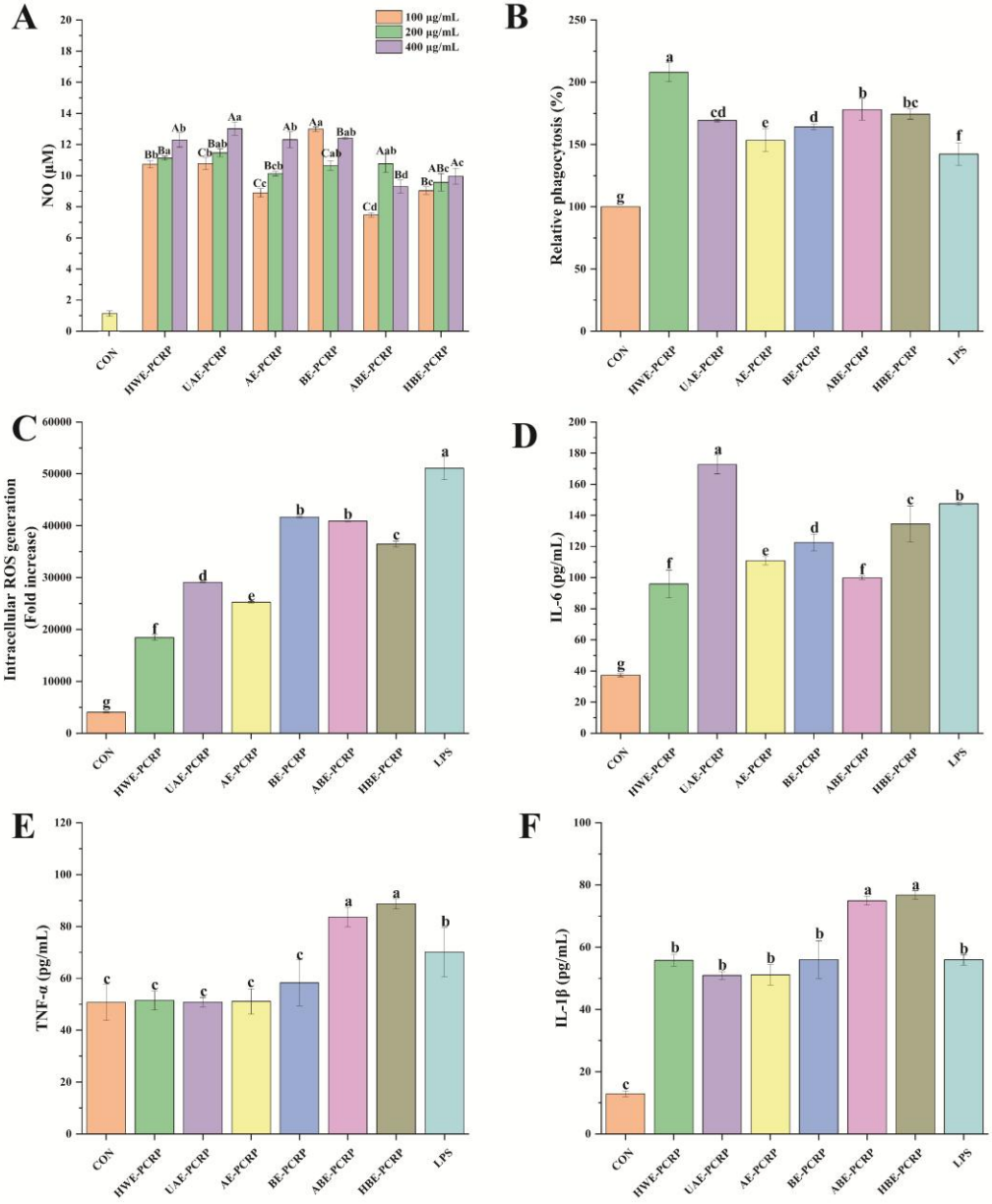

Fig.7 Effect of PcRPs on RAW 264.7 cells.

(A) NO production, (B) Phagocytic capacity, (C) ROS, (D) IL-6, (E) TNF-α, (F) IL-1β release from RAW 264.7 cells.

Different lowercase letters indicate significant differences between different groups ($P < 0.05$).

From a structural perspective, the superior immunomodulatory activity of HBE-PcRPs may be attributed to its relatively high uronic acid content (3.64%), parameters that have been associated with enhanced binding affinity to Toll-like receptor 4 (TLR4) on macrophage membranes in previous studies [65]. Wang et al. (2025) reported that acidic polysaccharides from steamed *Polygonatum cyrtonema*, triggered the phosphorylation of p38, ERK1/2, JNK, IκBα, and p65 via TLR4 upregulation, with the acidic polysaccharide fraction D3 exhibiting the most potent immunostimulatory effects. The authors further proposed that uronic acids, as key structural motifs in acidic polysaccharides, facilitate recognition by macrophage receptors such as TLR4, thereby enhancing phagocytosis and cytokine production. Analogously, the carboxylate moieties of uronic acid residues in HBE-P may likewise promote such receptor-mediated immune activation [66]. Additionally, the presence of β-glycosidic linkages could facilitate recognition by dectin-1 receptors, initiating downstream MAPK and NF-κB signaling cascades [67]. The observed dose-dependent increase in NO, ROS, and pro-inflammatory cytokines (IL-6, TNF-α, IL-1β) is consistent with this hypothetical pathway. However, direct experimental validation through WB and qPCR remains to be conducted in future studies.

In this study, the phenolic compounds refer to the total phenolic content (TPC) determined by the Folin–Ciocalteu method. PcRPs still contained phenolic compounds or other impurities, potentially interfering with structural characterization and functional activity results. In the future, more refined preparation processes will be established for the PcRP obtained through the optimal extraction method that has been selected. In particular, a variety of methods will be employed to control and ensure the purity of the polysaccharides.

In summary, the six polysaccharides (PcRPs) possessed distinct monosaccharide molar ratios, Mw, chain conformations, and microstructures, which in turn dictated their functional and bioactive profiles. HBE-PcRP extracted by HBE method had the highest Mw and the most favorable combination of anti-oxidant and immunomodulatory activities, positioning it as a promising ingredient for functional foods and feed additives, whereas the UAE method and the AE method preferentially

enhanced water/oil-holding and emulsifying performance, respectively. These findings underscore that the extraction method is a critical factor for tailoring PcR-derived polysaccharides toward target applications. The immunostimulatory activity of HBE-PcRP indicates its potential as a functional feed additive for livestock or aquaculture. Combined with the high yield of AE-PcRP and the hydration properties of UAE-PcRP, these results provide a valorization route for converting PcR into value-added polysaccharide products.These proposed applications highlight the practical utility of tailoring extraction protocols to obtain polysaccharides with desired food-related properties. These findings provide a foundation for establishing quantitative structure–activity relationships of PcRPs and highlight HBE-P as a promising candidate for functional food applications. Nevertheless, the precise molecular mechanisms underlying the immunomodulatory effects of PcRPs particularly the involvement of TLR4/MAPK/NF-κB signaling pathways remain to be experimentally verified. Future studies employing Western blot, quantitative real-time PcR, and pathway inhibition assays, as well as in vivo animal models, are necessary to validate the mechanistic hypotheses proposed herein and to fully realize the potential of PcRPs in nutraceutical development.

Abbreviations Used

PcRP, *P. citrinopileatus* residue polysaccharide; HWE, hot water extraction; UAE, ultrasound-assisted extraction; AE, acid-assisted extraction; BE, alkali-assisted extraction; ABE, sequential acid-alkali extraction; HBE, hot alkali extraction; WHC, water-holding capacity; OHC, oil-holding capacity; EAI, emulsification activity index; ESI, emulsifying stability index; FT-IR, Fourier-transform infrared spectroscopy; SEM, scanning electron microscopy; XRD, X-ray diffraction; TG, thermogravimetric; DTG, differential thermogravimetry; DSC, differential scanning calorimetry; DPPH, 1,1-diphenyl-2-picrylhydrazyl;ABTS,2,2'-azino-bis(3-ethylbenzothiazoline-6-sulfonic acid); NO, nitric oxide; IL-6, interleukin-6; TNF-α, tumor necrosis factor-α; IL-1β, interleukin-1β; LPS, lipopolysaccharide; PBS, phosphate-buffered saline; DMEM, Dulbecco's Modified Eagle Medium; FBS, fetal bovine serum; CCK-8, Cell Counting

Kit-8; DCFH-DA, 2',7'-dichlorodihydrofluorescein diacetate; ROS, reactive oxygen species; PDI, polydispersity index; Mw, molecular weight; Man, Mannose; GlcA, Glucuronic acid; Rha, Rhamnose; GalA, Galacturonic acid; Glc, Glucose; Gal, Galactose; Xyl, Xylose; Ara, Arabinose; Fuc, Fucose.

References

(1) Chen, J. N.; Wang, Y. T.; Wu, J. S. A Glycoprotein Extracted from Golden Oyster Mushroom *Pleurotus citrinopileatus* Exhibiting Growth Inhibitory Effect Against U937 Leukemia Cells. *J. Agric. Food. Chem.* **2009**, *57*, 6706-6711. Doi: 10.1021/jf901284s.

(2) Chen, J. N.; Tseng, M. C. T. P.; et al. *In Vitro* Anti-tumor and Immunomodulatory Effects of the Protein PCP-3A from Mushroom *Pleurotus Citrinopileatus*. J. Agric. Food Chem.2010, 58(23):12117-22. Doi: 10.1021/jf103576r.

(3) Meng, T.; Ishikawa, H.; Shimizu, K.; Ohga, S.; Kondo, R. A Glucosylceramide with Anti-microbial Activity from The Edible Mushroom *Pleurotus Citrinopileatus*. *J. Wood Sci.* **2012**, *58*, 81-86. Doi:10.1007/s10086-011-1213-y.

(4) Zhang, J.; Wang, G.; Li, H.; Zhuang, C.; Mizuno, T.; Ito, H.; Suzuki, C.; Okamoto, H.; Li, J. Anti-tumor Polysaccharides from A Chinese Mushroom, "Yuhuangmo," The Fruiting Body of *Pleurotus Citrinopileatus*. *Biosci. Biotechnol. Biochem.* **1994**, *58*, 1195-1201. Doi: 10.1271/bbb.58.1195.

(5) Meng, M.; Sun, Y.; Bai, Y.; Xu, J.; Sun, J.; Han, L.; Sun, H.; Han, R. A Polysaccharide from *Pleurotus Citrinopileatus* Mycelia Enhances The Immune Response in Cyclophosphamide-Induced Immunosuppressed Mice Via p62/Keap1/Nrf2 Signal Transduction Pathway. *Int. J. Biol. Macromol.* **2023**, *228*, 165-177. Doi: 10.1016/j.ijbiomac.2022.12.142.

(6) Deng, L.; Huang, G. Ultrasound-assisted Extraction, Optimization, Characteristics and Anti-oxidant Activity of *Piper Nigrum* L. Polysaccharides. *Ultrason. Sonochem.* **2025**, *116*, 107309. Doi: 10.1016/j.ultsonch.

(7) Li, R.; Wang, H.; Wang, Q.; Zhang, Z.; Wang, L. Acid-assisted Polysaccharides Extracted from *Asparagus Cochinchinensis* Protect Against Alzheimer's Disease by Regulating The

637 Microbiota-Gut-Brain Axis. *Front. Nutr.* **2024**, *11*, 1496306. Doi: 10.3389/fnut.
638 (8) Xiao, W.; Zhou, P.; Wang, X.; Zhao, R.; Wang, Y. Comparative Characterization and
639 Immunomodulatory Activities of Polysaccharides Extracted from the Radix of *Platycodon*
640 *grandiflorum* with Different Extraction Methods. *Molecules* **2022**, *27*, 4759. Doi:
641 10.3390/molecules27154759.
642 (9) Jiao, J.; Deng, P.; Peng, L.; Peng, C.; Jia, X.; Silviya, L. R.; Wang, X.; Dong, X. Current
643 Emerging Trends in Structure and Bioactivities of Acidic and Alkali-Extracted
644 Polysaccharides: A Review. *Ind. Crop. Prod.* **2026**, *243*, 123150. Doi:
645 10.1016/j.indcrop.2026.123150
646 (10) Tang, Y.; Wei, Z.; He, X.; Ling, D.; Qin, M.; Yi, P.; Liu, G.; Li, L.; Li, C.; Sun, J. A Comparison
647 Study on Polysaccharides Extracted from Banana Flower Using Different Methods:
648 Physicochemical Characterization, and Anti-oxidant and Anti-hyperglycemic Activities. *Int. J.*
649 *Biol. Macromol.* **2024**, *264*, 130459. Doi: 10.1016/j.ijbiomac.2024.130459.
650 (11) Jiao, X.; Li, F.; Zhao, J.; Wei, Y.; Zhang, L.; Wang, H.; Yu, W.; Li, Q. Structural Diversity and
651 Physicochemical Properties of Polysaccharides Isolated From Pumpkin (*Cucurbita Moschata*)
652 by Different Methods. *Food Res. Int.* **2023**, *163*, 112157. Doi: 10.1016/j.foodres.2022.112157.
653 (12) Nie, X. R.; Li, H. Y.; Du, G.; Lin, S.; Hu, R.; Li, H. Y.; Zhao, L.; Zhang, Q.; Chen, H.; Wu, D.
654 T.et al. Structural Characteristics, Rheological Properties, and Biological Activities of
655 Polysaccharides from Different Cultivars of Okra (*Abelmoschus Esculentus*) Collected in
656 China. *Int. J. Biol. Macromol.* **2019**, *139*, 459-467. Doi: 10.1016/j.ijbiomac.2019.08.016.
657 (13) Li, H.; Liu, S.; Liu, Y.; Li, W.; Niu, A.; Ren, P.; Liu, Y.; Jiang, C.; Inam, M.; Guan, L. Effects of
658 *In Vitro* Digestion and Fermentation of *Nostoc Commune Vauch* Polysaccharides on Properties
659 and Gut Microbiota. *Carbohydr. Polym.* **2022**, *281*, 119055. Doi: 10.1016/j.carbpol.
660 (14) Liu, Y.; Sun, Y.; Li, H.; Ren, P.; Inam, M.; Liu, S.; Liu, Y.; Li, W.; Niu, A.; Liu, S.et al.
661 Optimization of Ultrasonic Extraction of Polysaccharides from *Flammulina Velutipes* Residue
662 and Its Protective Effect Against Heavy Metal Toxicity. *Ind. Crop. Prod.* **2022**, *187*, 115422.
663 Doi: doi.org/10.1016/j.indcrop.2022.115422
664 (15) Nie, C.; Zhu, P.; Ma, S.; Wang, M.; Hu, Y. Purification, Characterization And
665 Immunomodulatory Activity Of Polysaccharides From *Stem Lettuce*. *Carbohydr. Polym.* **2018**,
666 *188*, 236-242. Doi: 10.1016/j.carbpol..2018.02.009.

(16) Lv, Y.; Yao, L.; Qiu, M.; Li, L.; Qiu, S.; Liu, Y.; Wei, C. Physicochemical Properties, Structural Characteristics and Bioactivities of *Pyracantha Fortuneana* Polysaccharides Prepared by Six Methods. *Ind. Crop. Prod.* **2024**, *208*, 117933. Doi:10.1016/j.indcrop.2023.117933

(17) Alpizar-Reyes, E.; Carrillo-Navas, H.; Gallardo-Rivera, R.; Varela-Guerrero, V.; Alvarez-Ramirez, J.; Pérez-Alonso, C. Functional Properties and Physicochemical Characteristics of Tamarind (*Tamarindus Indica l.*) Seed Mucilage Powder as a Novel Hydrocolloid. *J. Food Eng.* **2017**, *209*, 68-75. Doi:10.1016/j.jfoodeng.2017.04.021

(18) Einhorn-Stoll, U.; Kunzek, H.; Dongowski, G. Thermal Analysis of Chemically and Mechanically Modified Pectins. *Food Hydrocoll.* **2007**, *21*, 1101-1112. Doi:10.1016/j.foodhyd.2006.08.004

(19) Li, X.; Qu, D.; Sha, J.; Sun, Y. A Comparative Study on Physicochemical and Emulsifying Properties of White and *Red Ginseng* Dietary Fibers From *Ginseng* Residues. *Lwt* **2024**, *208*, 116729. Doi:10.1016/j.lwt.2024.116729

(20) Wang, L.; Li, Y.; Ye, L.; Zhi, C.; Zhang, T.; Miao, M. Pu-Erh Tea-Derived Cellulose Exhibits Superior Water/Oil Holding Capacity Compared to Black and Green Tea Celluloses: A Comprehensive Analysis. *Food Biosci.* **2024**, *59*, 104073. Doi:10.1016/j.fbio.2024.104073

(21) Wang, L.; Chen, C.; Zhang, B.; Huang, Q.; Fu, X.; Li, C. Structural Characterization Of a Novel Acidic Polysaccharide From *Rosa Roxburghii Tratt* Fruit And Its Alpha-Glucosidase Inhibitory Activity. *Food Funct.* **2018**, *9*, 3974-3985. Doi: 10.1039/c8fo00561c.

(22) Yang, Y.; Zhang, X.; Zhang, J.; Wang, T.; Liu, S.; Ma, H.; Inam, M.; Guan, L. Green Ultrasonic-Assisted Enzymatic Extraction Of Polysaccharides From *Flammulina Velutipes* Residues By Response Surface Methodology. *Sustain. Chem. Pharm.* **2024**, *41*, 101690. Doi:10.1016/j.scp.2024.101690

(23) Hu, S.; Y. J. G. J. Anti-oxidant and Anti-Inflammatory Potential of Peptides Derived from *In Vitro* Gastrointestinal Digestion of Germinated and Heat-Treated Foxtail Millet (*Setaria italica*) Proteins. *J. Agric. Food. Chem.* **2020**, *2;68(35):9415-9426*. Doi: 10.1021/acs.jafc.0c03732.

(24) Yang, Y.; Ren, P.; Sun, Y.; Li, J.; Zhou, X.; Zhang, H.; He, C.; Dai, H.; Guan, L. Structure Elucidation and Molecular Mechanism of An Immunomodulatory Polysaccharide from *Nostoc Commune*. *Int. J. Biol. Macromol.* **2024**, *283*, 137435. Doi: 10.1016/j.ijbiomac.2024.137435.

(25) Laiqing Deng, G. H. Ultrasound-Assisted Extraction, Optimization, Characteristics and

Anti-oxidant Activity of *Piper Nigrum l.* Polysaccharides. *Ultrason. Sonochem.* **2025**. Doi: 10.1016/j.ultsonch.2025.107309.

(26) Leong, Y. K.; Yang, F.; Chang, J. Extraction of Polysaccharides from Edible Mushrooms: Emerging Technologies and Recent Advances. *Carbohydr. Polym.* **2021**, *251*, 117006. Doi: 10.1016/j.carbpol.2020.117006.

(27) Chi, Y.; Li, Y.; Zhang, G.; Gao, Y.; Ye, H.; Gao, J.; Wang, P. Effect of Extraction Techniques on Properties of Polysaccharides from *Enteromorpha Prolifera* and Their Applicability in Iron Chelation. *Carbohydr. Polym.* **2018**, *181*, 616-623. Doi: 10.1016/j.carbpol.2017.11.104.

(28) Zhang, D.; Wan, Y.; Xu, J.; Wu, G.; Li, L.; Yao, X. Ultrasound Extraction of Polysaccharides from Mulberry Leaves and Their Effect on Enhancing Anti-oxidant Activity. *Carbohydr. Polym.* **2016**, *137*, 473-479. Doi: 10.1016/j.carbpol.2015.11.016.

(29) Wu, M.; Li, W.; Zhang, Y.; Shi, L.; Xu, Z.; Xia, W.; Zhang, W. Structure Characteristics, Hypoglycemic and Immunomodulatory Activities of Pectic Polysaccharides from *Rosa Setate* x *Rosa Rugosa* Waste. *Carbohydr. Polym.* **2021**, *253*, 117190. Doi: 10.1016/j.carbpol.2020.117190.

(30) Dong, K.; Wang, J.; Tang, F.; Liu, Y.; Gao, L. A Polysaccharide with a Triple Helix Structure from *Agaricus Bisporus*: Characterization and Anti-Colon Cancer Activity. *Int. J. Biol. Macromol.* **2024**, *281*, 136521. Doi: 10.1016/j.ijbiomac.2024.136521.

(31) Zheng, M.; Ma, M.; Yang, Y.; Liu, Z.; Liu, S.; Hong, T.; Ni, H.; Jiang, Z. Structural Characterization and Anti-oxidant Activity of Polysaccharides Extracted from *Porphyra Haitanensis* by Different Methods. *Int. J. Biol. Macromol.* **2023**, *242*, 125003. Doi: 10.1016/j.ijbiomac.2023.125003.

(32) Wang, Z.; Zheng, Y.; Lai, Z.; Hu, X.; Wang, L.; Wang, X.; Li, Z.; Gao, M.; Yang, Y.; Wang, Q.et al. Effect of Monosaccharide Composition and Proportion on The Bioactivity of Polysaccharides: a Review. *Int. J. Biol. Macromol.* **2024**, *254*, 127955. Doi: 10.1016/j.ijbiomac.2023.127955.

(33) Yi, J.; Li, X.; Wang, S.; Wu, T.; Liu, P. Steam Explosion Pretreatment of *Achyranthis Bidentatae* Radix: Modified Polysaccharide and Its Anti-oxidant Activities. *Food Chem.* **2022**, *375*, 131746. Doi: 10.1016/j.foodchem.2021.131746.

(34) Han, B.; Baruah, K.; Cox, E.; Vanrompay, D.; Bossier, P. Structure-Functional Activity

Relationship of β-Glucans from the Perspective of Immunomodulation: A Mini-Review. *Front. Immunol.* **2020**, *Volume 11 - 2020*. Doi: 10.3389/fimmu.2020.00658. eCollection 2020.

(35) He, L.; Yan, X.; Liang, J.; Li, S.; He, H.; Xiong, Q.; Lai, X.; Hou, S.; Huang, S. Comparison of Different Extraction Methods for Polysaccharides from *Dendrobium Officinale* Stem. *Carbohydr. Polym.* **2018**, *198*, 101-108. Doi: 10.1016/j.carbpol.2018.06.073.

(36) Zhao, Z.; Wang, L.; Ruan, Y.; Wen, C.; Ge, M.; Qian, Y.; Ma, B. Physicochemical Properties and Biological Activities of Polysaccharides from The Peel of *Dioscorea Opposita Thunb*. Extracted by Four Different Methods. *Food Sci. Human Wellness* **2023**, *12*, 130-139. Doi:10.1016/j.fshw.2022.07.031

(37) Peasura, N.; Laohakunjit, N.; Kerdchoechuen, O.; Wanlapa, S. Characteristics and Anti-oxidant of Ulva Intestinalis Sulphated Polysaccharides Extracted with Different Solvents. *Int. J. Biol. Macromol.* **2015**, *81*, 912-919. Doi: 10.1016/j.ijbiomac.2015.09.030.

(38) Wang, S.; Zhao, L.; Li, Q.; Liu, C.; Han, J.; Zhu, L.; Zhu, D.; He, Y.; Liu, H. Rheological Properties and Chain Conformation of Soy Hull Water-Soluble Polysaccharide Fractions Obtained by Gradient Alcohol Precipitation. *Food Hydrocoll.* **2019**, *91*, 34-39. Doi:10.1016/j.foodhyd.2018.12.054

(39) Qiu, C.; Wang, B.; Wang, Y.; Teng, Y. Effects of Colloidal Complexes Formation between Resveratrol and Deamidated Gliadin on The Bioaccessibility and Lipid Oxidative Stability. *Food Hydrocoll.* **2017**, *69*, 466-472. Doi:10.1016/j.foodhyd.2017.02.020

(40) Gu, J.; Zhang, H.; Yao, H.; Zhou, J.; Duan, Y.; Ma, H. Comparison of Characterization, Anti-oxidant and Immunological Activities of Three Polysaccharides from *Sagittaria Sagittifolia l*. *Carbohydr. Polym.* **2020**, *235*, 115939. Doi: 10.1016/j.carbpol.2020.115939.

(41) Yan, Y.; Li, X.; Wan, M.; Chen, J.; Li, S.; Cao, M.; Zhang, D. Effect of Extraction Methods on Property and Bioactivity of Water-Soluble Polysaccharides from *Amomum Villosum*. *Carbohydr. Polym.* **2015**, *117*, 632-635. Doi: 10.1016/j.carbpol.2014.09.070.

(42) Vanloot, P.; Dupuy, N.; Guiliano, M.; Artaud, J. Characterisation and Authentication of *A. Senegal* And *A. Seyal* Exudates by Infrared Spectroscopy and Chemometrics. *Food Chem.* **2012**, *135*, 2554-2560. Doi: 10.1016/j.foodchem.2012.06.125.

(43) Yan, J.; Ding, Z.; Gao, X.; Wang, Y.; Yang, Y.; Wu, D.; Zhang, H. Comparative Study of Physicochemical Properties and Bioactivity of *Hericium Erinaceus* Polysaccharides at

Different Solvent Extractions. *Carbohydr. Polym.* **2018**, *193*, 373-382. Doi: 10.1016/j.carbpol.2018.04.019.

(44) Abuduwaili, A.; Nuerxiati, R.; Mutailifu, P.; Gao, Y.; Lu, C.; Yili, A. Isolation, Structural Modification, Characterization, and Bioactivity of Polysaccharides from *Folium Isatidis*. *Ind. Crop. Prod.* **2022**, *176*, 114319. Doi: 10.1016/j.indcrop.2021.114319

(45) Qian, J.; Chen, W.; Zhang, W.; Zhang, H. Adulteration Identification of Some Fungal Polysaccharides with Sem, Xrd, Ir and Optical Rotation: A Primary Approach. *Carbohydr. Polym.* **2009**, *78*, 620-625. Doi: 10.1016/j.carbpol.2009.05.025

(46) Wang, Y.; Li, X.; Chen, X.; Zhao, P.; Qu, Z.; Ma, D.; Zhao, C.; Gao, W. Effect of Stir-Frying Time during *Angelica Sinensis* Radix Processing with Wine on Physicochemical, Structure Properties and Bioactivities of Polysaccharides. *Process Biochem.* **2019**, *81*, 188-196. Doi: 10.1016/j.procbio.2019.02.020

(47) Gong, L. L.; Meng, F. J.; Hou, Y. C.; Liu, Y.; Xu, J. J.; Zhang, W. N.; Chen, Y. Purification, Characterization, and Bioactivity of Two New Polysaccharide Fractions from *Thelephora Ganbajun* Mushroom. *J. Food Biochem.* **2020**, *44*, e13092. Doi: 10.1111/jfbc.13092.

(48) Ma, F.; Wang, D.; Zhang, Y.; Li, M.; Qing, W.; Tikkanen-Kaukanen, C.; Liu, X.; Bell, A. E. Characterisation of The Mucilage Polysaccharides from *Dioscorea Opposita Thunb.* with Enzymatic Hydrolysis. *Food Chem.* **2018**, *245*, 13-21. Doi: 10.1016/j.foodchem.2017.10.080.

(49) Fan, R.; Mao, G.; Xia, H.; Zeng, J. Chemical Elucidation and Rheological Properties of a Pectic Polysaccharide Extracted from *Citrus Medica l.* Fruit Residues by Gradient Ethanol Precipitation. *Int. J. Biol. Macromol.* **2022**, *198*, 46-53. Doi: 10.1016/j.ijbiomac.2021.12.131.

(50) Chang, L.; Kong, B.; Liu, Q.; Du, X.; Xia, X. Effect of Freeze-Thaw Processes on The Water-Absorption Ability and Mechanical Properties of Hydrogel Pads with Chitosan/Poly(Vinyl Alcohol) Based on Citrate Crosslinks. *Food Chem.* **2025**, *471*, 142785.Doi: 10.1016/j.foodchem.2025.142785.

(51) Chen, H.; Huang, Y.; Zhou, C.; Xu, T.; Chen, X.; Wu, Q.; Zhang, K.; Li, Y.; Li, D.; Chen, Y. Effects of Ultra-High Pressure Treatment on Structure and Bioactivity of Polysaccharides from Large Leaf Yellow Tea. *Food Chem.* **2022**, *387*, 132862. Doi: 10.1016/j.foodchem.2022.132862.

(52) Chen, Y.; Xue, Y. Purification, Chemical Characterization and Anti-oxidant Activities of a

Novel Polysaccharide from *Auricularia Polytricha*. *Int. J. Biol. Macromol.* **2018**, *120*, 1087-1092. Doi: 10.1016/j.ijbiomac.2018.08.160.

(53) Kittur, F. S.; Harish Prashanth, K. V.; Udaya Sankar, K.; Tharanathan, R. N. Characterization of Chitin, Chitosan and Their Carboxymethyl Derivatives by Differential Scanning Calorimetry. *Carbohydr. Polym.* **2002**, *49*, 185-193. Doi:10.1016/S0144-8617(01)00320-4

(54) Mohammed, J. K.; Mahdi, A. A.; Ahmed, M. I.; Ma, M.; Wang, H. Preparation, Deproteinization, Characterization, and Anti-oxidant Activity of Polysaccharide from *Medemia Argun* Fruit. *Int. J. Biol. Macromol.* **2020**, *155*, 919-926.Doi: 10.1016/j.ijbiomac.2019.11.050.

(55) Sun, C.; Chen, S.; Dai, L.; Gao, Y. Structural Characterization and Formation Mechanism of Zein-Propylene Glycol Alginate Binary Complex Induced by Calcium Ions. *Food Res. Int.* **2017**, *100*, 57-68. Doi: 10.1016/j.foodres.2017.08.022.

(56) Song, Q.; Jiang, L.; Yang, X.; Huang, L.; Yu, Y.; Yu, Q.; Chen, Y.; Xie, J. Physicochemical and Functional Properties of A Water-Soluble Polysaccharide Extracted from Mung Bean (*Vigna Radiate l.*) and Its Anti-oxidant Activity. *Int. J. Biol. Macromol.* **2019**, *138*, 874-880. Doi: 10.1016/j.ijbiomac.2019.07.167.

(57) Chen, X.; Wang, Z.; Kan, J. Polysaccharides from *Ginger Stems* and Leaves: Effects of Dual and Triple Frequency Ultrasound Assisted Extraction on Structural Characteristics and Biological Activities. *Food Biosci.* **2021**, *42*, 101166. Doi:10.1016/j.fbio.2021.101166

(58) Funami, T.; Nakauma, M.; Ishihara, S.; Tanaka, R.; Inoue, T.; Phillips, G. O. Structural Modifications of Sugar Beet Pectin and The Relationship of Structure to Functionality. *Food Hydrocoll.* **2011**, *25*, 221-229. Doi:10.1016/j.foodhyd.2009.11.017

(59) Zhang, C.; Zhao, F.; Li, R.; Wu, Y.; Liu, S.; Liang, Q. Purification, Characterization, Anti-oxidant and Moisture-Preserving Activities of Polysaccharides from *Rosa Rugosa Petals*. *Int. J. Biol. Macromol.* **2019**, *124*, 938-945. Doi: 10.1016/j.ijbiomac.2018.11.275.

(60) Li, X.; Wang, L.; Wang, Y.; Xiong, Z. Effect of Drying Method on Physicochemical Properties and Anti-oxidant Activities of *Hohenbuehelia Serotina* Polysaccharides. *Process Biochem.* **2016**, *51*, 1100-1108. Doi:10.1016/j.procbio.2016.05.006

(61) Wang, M.; Zhu, P.; Zhao, S.; Nie, C.; Wang, N.; Du, X.; Zhou, Y. Characterization, Anti-oxidant Activity and Immunomodulatory Activity of Polysaccharides from The Swollen

Culms of *Zizania Latifolia*. *Int. J. Biol. Macromol.* **2017**, *95*, 809-817. Doi: 10.1016/j.ijbiomac.2016.12.010.

(62) Mohanta, B.; Sen, D. J.; Mahanti, B.; Nayak, A. K. Extraction, Characterization, Haematocompatibility and Anti-oxidant Activity of Linseed Polysaccharide. *Carbohydrate Polymer Technologies and Applications* **2023**, *5*, 100321. Doi: 10.1016/j.carpta.2023.100321

(63) Chen, D.; Kang, Z.; Chen, H.; Fu, P. Molecular Mechanisms of Macrophage Immunomodulation Mediated by Areca Inflorescence Polysaccharides Based on Rna-Seq Analysis. *Int. J. Biol. Macromol.* **2024**, *263*, 130076. Doi: 10.1016/j.ijbiomac.2024.130076.

(64) Zhang, L.; Wang, Q.; Gao, N.; Lin, G.; Hu, D.; Liu, J.; Wang, J.; Zhao, S.; Zhang, J.; Zheng, T.et al. The Study on *In Vitro* Anti-oxidant Properties, Cellular Immune Activities and Mice Anti-Fatigue Effects of *Sanghuangporus Vanninii* Mycelium Polysaccharides. *Food Biosci.* **2024**, *61*, 104640. Doi:10.1016/j.fbio.2024.104640

(65) Liao, Q.; He, Y.; Wu, C.; Deng, Z.; Liu, J. Hawthorn Fruit (*Crataegus Spp.*) Polysaccharides Exhibit Immunomodulatory Activity on Macrophages Via Tlr4/Nf-Kappab Signaling Activation. *Plant Food Hum. Nutr.* **2024**, *79*, 367-373. Doi: 10.1007/s11130-024-01160-3.

(66) Wang, Y.; Wu, L.; Zhang, Y.; Tan, Q.; Huang, S.; Li, Y.; Wang, H.; Chen, C.; Wu, W. Three New Acidic Polysaccharides from Steamed *Polygonatum Cyrtonema Hua* Modulate Immunomodulatory Activities Via Tlr4-Mediated Mapk and Nf-Kb Pathways. *Food Biosci.* **2025**, *74*, 107935. Doi:10.1016/j.fbio.2025.107935

(67) Zhang, R.; Xiong, Y.; Ma, Y.; Ma, Y.; Li, N.; Ren, Y.; He, L.; Han, L.; Ni, J.; Yuan, Z. *Asparagus Officinalis* Polysaccharide-Loaded Liposomal Gels Alleviate Skin Inflammation Via Inhibiting The Nf-Kb/Mapk Pathways. *J. Funct. Foods* **2025**, *125*, 106679. Doi:10.1016/j.jff.2025.106679

Statements and Declarations

Conflict of Interest

The authors declare no competing financial interest.

Funding Sources

This work was supported by Jilin Provincial Scientific and Technological Development Program (grant number 20240101247JC).

Author Contributions

Kunpeng Lu: Conceptualization, Writing-Original Draft, Validation, Writing-Review & Editing.

Yao Zhang: Conceptualization, Methodology, Writing-Original Draft, Writing-Review & Editing.

Xinran Liu: Formal analysis, Supervision, Validation.

Linna Du: Methodology, Supervision, Writing-Review & Editing.

Yuting Li: Conceptualization, Methodology, Formal analysis, Supervision, Writing-review & editing.

Lili Guan: Conceptualization, Methodology, Formal analysis, Supervision, Writing-review & editing.

Acknowledgments

We sincerely thank Dr. Muhammad Inam for his expert linguistic refinement of this manuscript.

Data Availability

The datasets generated during the current study are available from the corresponding author on reasonable request.

Supplementary Files

This is a list of supplementary files associated with this preprint. Click to download.

- AuthorContributions.docx
- ConflictofInterest.docx
- DeclarationofInterestStatement.docx
- FundingSources.docx
- Highlights.docx
- SupportingInformationforPublication.docx